

Absorption, Reflectance, and Luminescence of GaN Epitaxial Layers

R. Dingle, D. D. Sell, S. E. Stokowski, and M. Ilegems

Bell Telephone Laboratories, Murray Hill, New Jersey 07974

(Received 23 March 1971)

Low-temperature absorption, reflectance, and emission spectra from a wide range of epitaxially grown GaN are reported. The best samples, which are far superior to any previously available, have spectral details that allow a definitive analysis. The reflectance results prove that GaN is a direct-gap semiconductor with its lowest exciton state at 3.474 ± 0.002 eV at 2 K. The absorption and luminescence spectra corroborate this observation. Crystal field and spin-orbit splittings have been resolved. The order of the valence-band states is $\Gamma_9 > \Gamma_7 > \Gamma_7$ with parameters $\Delta_{c,r} = 22 \pm 2$ meV and $\Delta_{s,o} = 11 \pm 2$ meV. A correlation of these results with the emission data has led us to an interpretation in which we associate emission features with LO-phonon-assisted free-exciton decay, with bound-exciton decay at both donor and acceptor sites, and with distant donor-acceptor pair recombination. Binding energies derived from these associations are consistent with values obtained from independent experiments reported earlier. The internal consistency of the absorption, reflectance, and luminescence results provides strong support for our interpretation.

I. INTRODUCTION

In an earlier publication,¹ we discussed the absorption, reflectance, and luminescence of single-crystal needles of highly n -type GaN. These crystals were subsequently used to demonstrate the presence of stimulated emission and laser action at ~ 3.45 eV in GaN.² As pointed out in the original paper, the high concentration of free electrons in these needles, $n > 10^{19}$ cm⁻³, had a drastic effect upon the breadth of the absorption, emission, and reflectivity structure. As a result of this broadening, we were not able to resolve any fine structure in the spectra and a detailed discussion of the electronic structure of GaN could not be given. At that time, we also indicated that attempts to improve the quality of the GaN at our disposal were continuing. Indeed, without such improvements we could not hope to gain a better understanding of its electronic properties.

The present paper reports more recent spectral measurements made on a wide range of epitaxial layers of GaN grown on (0001) sapphire. With this method of growth (Sec. II) we have reduced the room-temperature, free-electron concentration by more than two orders of magnitude from that found in the needles. At these concentrations ($n \sim 10^{17}$ cm⁻³), sharp and detailed reflectance and luminescence have been observed. The absorption data also sharpen somewhat and shift to lower energies from those observed in the needles. Moreover, we have been able to measure the three distinct polarizations in reflectance and luminescence.

The reflectance (Sec. IV) and absorption (Sec. III) results, which bear mostly upon the intrinsic properties of these epitaxial layers of GaN, provide strong evidence for a direct fundamental gap

with the lowest free-exciton transition at 3.474 ± 0.002 eV (at 2 K). The structure immediately above this energy, and the over-all polarization of the reflectance data, have been analyzed to show that the transitions occur at (or near) $k=0$. The valence band is split by crystal field and spin-orbit effects into Γ_9 , Γ_7 , and Γ_7 states of C_{6v} . The order of these states is the "normal" order.³ Some of the finer details of the $E \perp c$, $k \parallel c$ reflectance spectrum are not totally understood at this time. Possible reasons for this are discussed.

Luminescence results (Sec. V) generally relate to the extrinsic properties of the layers. In addition, we have observed structure which we associate with LO-phonon-assisted decay of the 3.474-eV free exciton. From this and other observations, exciton binding energies, donor and acceptor binding energies, and recombination mechanisms are proposed. The consistency of these results gives us confidence in the general validity of our interpretation.

Throughout the course of this investigation we have observed a wide variety of reflectance, absorption, and luminescence spectra. To some degree this is expected since the crystal-growth parameters were varied in order to investigate their influence on the optical properties of the layers. In fact, the reflectance and luminescence spectra were used to monitor the quality of the samples at the same time as we were studying the spectra in order to understand the electronic structure of GaN.

To facilitate the cataloging of results, and the discussion of spectra from a large number of samples, we have set up empirical criteria that separate the data, and hence the layers, into three groups designated types I, II, and III. The reflectance

tance spectra of representative members of each group are shown in Fig. 1. Specifically, samples in which the three band-edge excitons are resolved in reflectance are designated type I. These layers have free-electron concentrations $\sim 10^{17} \text{ cm}^{-3}$, mobilities $> 300 \text{ cm}^2/\text{V sec}$, sharp luminescence, and are at least $100 \mu\text{m}$ thick. The bulk of this paper is concerned with these samples.

Type-II samples show strong, relatively sharp, but yet unresolved reflectance near 3.47 eV . In some cases a broader structure is seen near 3.6 eV . These layers have free-electron concentrations of $\sim 10^{18} \text{ cm}^{-3}$, mobilities of $< 100 \text{ cm}^2/\text{V sec}$ and are $5\text{--}20 \mu\text{m}$ thick. Absorption measurements were possible with such samples. Typically, the absorption has a strong broad maximum near 3.45 eV .

Other epitaxial layers that have broad, poorly resolved reflectance, luminescence, and absorption in the near uv are termed type-III layers. Electrical measurements on these samples indicate mobilities of $< 100 \text{ cm}^2/\text{V sec}$ and free-carrier concentrations $\geq 10^{19} \text{ cm}^{-3}$. Many of the properties of these type-III layers are indistinguishable from those of the needles. In particular, type-III layers exhibit only a weak reflectance near 3.47 eV . The reflectance tends to be dominated by structure near 3.6 eV similar to that reported earlier.¹

II. MATERIAL

The GaN samples were grown by vapor epitaxy on (0001)-oriented sapphire substrates. The va-

por-deposition apparatus consists of a 75-cm -long horizontal single-zone resistance-heated furnace containing a reaction tube through which a continuous flow of reagent and carrier gases is maintained. Two separate gas streams, containing, respectively, GaCl and NH_3 (99.999% nominal purity), both diluted in a He (99.995% nominal purity) carrier, arrive separately at the deposition zone. The GaCl is produced *in situ* by passing HCl gas (99.99% nominal purity) over a heated Ga (99.9999% nominal purity) charge. The reaction apparatus is made entirely of fused silica, with the exception of the boat containing the Ga charge for which either silica or alumina is used.

For all samples reported in this study, the reaction- and deposition-zone temperature was $(1050 \pm 10)^\circ\text{C}$. Flow rates were empirically adjusted for optimum growth conditions. Three to five substrates, each approximately 1 cm^2 in area, were used per run. These substrates were positioned lengthwise in the reaction tube, over an approximately 5-cm -long zone of essentially constant temperature. Mixing of the (GaCl + He) and (NH_3 + He) gas streams occurs at the upstream end of the above-defined deposition zone. Type-I layers were always grown on the first (upstream) substrate while the downstream-layer deposits were always type II or type III. Back-reflection Laue x-ray patterns taken on the thick ($\geq 100 \mu\text{m}$) type-I layers established that these were (0001)-oriented single crystals. The growth morphology of the thinner type-II and -III layers leaves no doubt that these too are (0001)-oriented single crystals. Further details on crystal growth will be presented elsewhere.⁴

III. ABSORPTION SPECTRA

Type-I layers were generally $100\text{--}250 \mu\text{m}$ thick. Absorption measurements in the exciton region could not be made. In Fig. 2 we show a selection of 2 K absorption spectra obtained from thin ($5\text{--}10\text{-}\mu\text{m}$) type-II layers. Several of these exhibit a well-resolved peak in the $3.43\text{--}3.47\text{-eV}$ range. On the assumption that $d \sim 5 \mu\text{m}$, which is the measured thickness of the layer responsible for the curve marked U7-3 in Fig. 2, the absorption coefficient α is $\geq 10^4 \text{ cm}^{-1}$ for all the layers in which the peak is resolved. Only $k \parallel c$ data could be obtained with the samples at our disposal.

The absorption bands near 3.45 eV are 50 meV or more in half-width, considerably greater than the width of the equivalent reflectance and luminescence bands in the same layers. The breadth of the absorption data is attributed to the fact that absorption is a bulk property, whereas reflectance and luminescence are dominated by a thin ($< 1 \mu\text{m}$) region near the surface. The lattice mismatch⁵ between sapphire and GaN is some 13% in a on

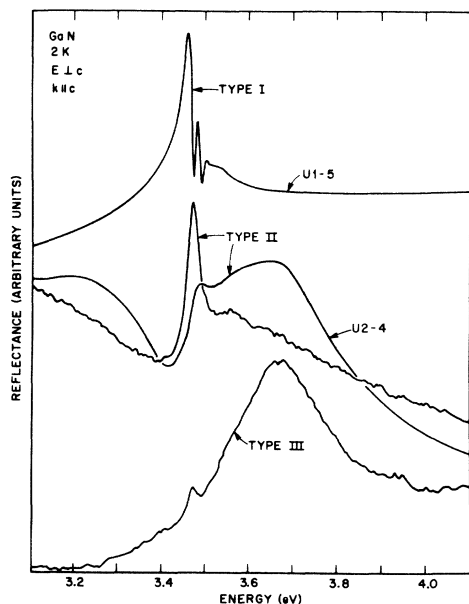


FIG. 1. Reflectance spectra ($E \perp c, k \parallel c$) at 2 K representing the three types of spectra observed for epitaxial layers of GaN on sapphire.

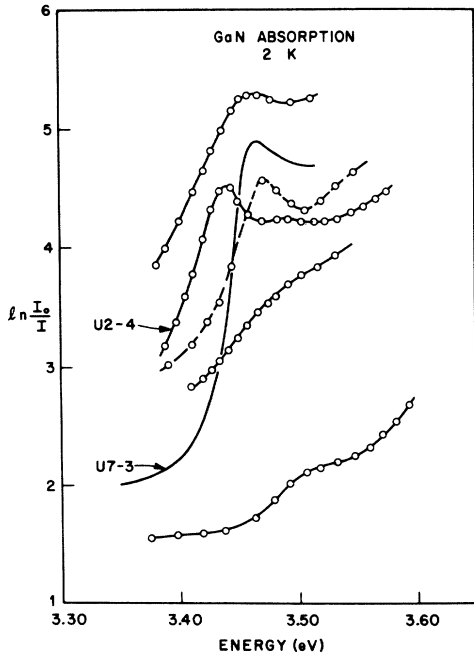


FIG. 2. Absorption data for thin type-II layers of GaN at 2 K. For the layers in which a peak is resolved, the absorption coefficient $\alpha > 10^4 \text{ cm}^{-1}$ (see text).

(0001) and is sufficient to strain badly the layer near the interface. This strain makes a dominant contribution to the broadening of the absorption spectra. Moreover, the fact that type-I layers are *always* thick may be attributed to the diminution of this lattice-mismatch strain as the upper surface is removed further from the substrate-layer interface.

Returning to Fig. 2, we observe that the peak near 3.45 eV is always $\leq 3.474 \text{ eV}$, which is the energy of the lowest exciton as observed in reflectance from type-I samples. This broadening and shift to lower energies may be related to the presence of shallow bound-exciton states immediately below the free exciton. It has been shown⁶ that such shallow extrinsic exciton states can have giant oscillator strengths, and if present in sufficient numbers, they can make significant contributions to the low-energy side of the intrinsic absorption edge. From the luminescence data we believe that bound-exciton levels exist 6–20 meV below the free-exciton energy, which is sufficient to account for the shifts seen in the spectra.

A particularly good illustration of this bound-exciton contribution to the near-band-gap absorption can be seen in Fig. 2, where the curve marked U2-4 has a well-defined maximum at 3.44 eV ($\alpha \approx 4 \times 10^4 \text{ cm}^{-1}$). The emission from this same crystal is dominated by a band which peaks at 3.43 eV (Fig. 6, marked U2-4), and the reflectance

(See Fig. 1) exhibits a broad anomaly in this range in addition to the sharp feature at 3.47 eV. Thus absorption, reflectivity, and emission appear to be dominated by this extrinsic phenomenon in this particular sample.

The type-II absorption data shown in Fig. 2 and discussed in this section give strong support to the notion that a direct, free-exciton transition occurs near 3.47 eV in epitaxial GaN. The observed strength and shape of the absorption are in good agreement with the theoretical predictions for a simple Wannier exciton.⁷ Furthermore, such a large absorption coefficient is at least an order-of-magnitude too large for an indirect transition.

IV. REFLECTANCE SPECTRA

The reflectance data for type-I layers are shown in Fig. 3. The data for $E \perp c$, $k \parallel c$ (α polarization) were obtained on as-grown surfaces. The data for $E \perp c$, $k \perp c$ (σ polarization) and $E \parallel c$, $k \perp c$ (π polarization) were obtained by breaking the substrates and films and looking at the irregularly cleaved edge of the layer.

The data were obtained with a double-beam spectrophotometer described previously.⁸ For 2 K operation, the samples were immersed in pumped liquid helium. The sensitivity and accuracy of the data were limited primarily by surface roughness and sample size (typically 1 mm^2). The absolute reflectance scale for α polarization has a negligi-

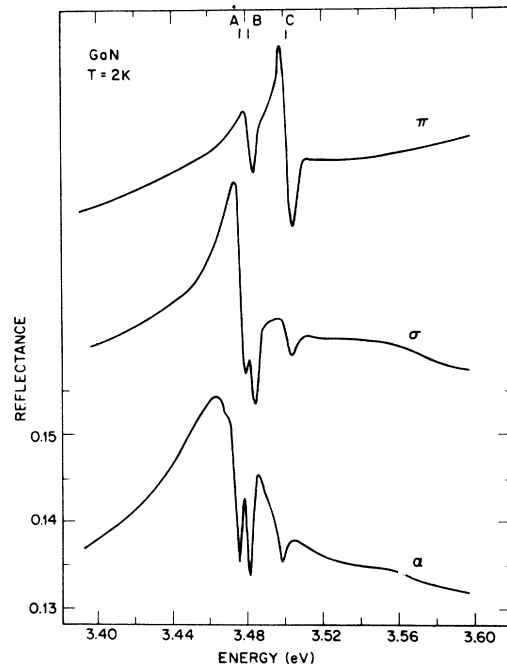


FIG. 3. Reflectance spectrum of type-I GaN at 2 K. The three polarizations are defined as follows: $\pi(E \parallel c, k \perp c)$, $\sigma(E \perp c, k \perp c)$, and $\alpha(E \perp c, k \parallel c)$.

ble additive error, but could have a multiplicative error as great as $\pm 30\%$. The σ and π data were somewhat more difficult to obtain. The light was focused upon the edge of the GaN layer which was generally only 100–150 μm thick. In this case, only a fraction of the light was specularly reflected and collected by the optical system. Consequently, it was not possible to maintain an absolute reflectance calibration. The vertical scale in Fig. 3 does not apply to the σ and π data.

For relatively flat surfaces (See the type-I data in Fig. 1), the noise corresponds to a reflectance of approximately 5×10^{-4} or less. For more inhomogeneous surfaces, which tend to be characteristic of types II and III (and the edges of type I), the noise (See Fig. 1) is greater owing to small vibrations of the optical beam relative to the sample.

Our data provide strong evidence that GaN has a direct fundamental band gap. An indirect transition could not give rise to such strong absorption and reflectance structure. In addition, the highest-energy luminescence peak at 3.467 ± 0.001 eV (2 K, type-I layers) is only a few millivolts below the lowest-energy reflectance structure. The energies of the reflectance and luminescence structure exhibit the same temperature dependence (predominant peaks for both are near 3.39 eV at 300 K). We believe this evidence provides conclusive proof that GaN has a direct fundamental band gap.

In all known cases, the III-V and II-VI semicon-

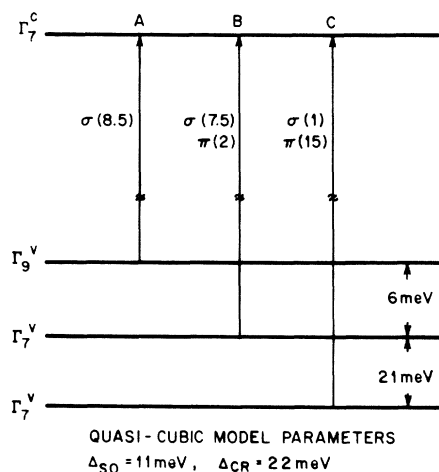


FIG. 4. Schematic representation of upper-valence- and lowest-conduction-band states at the Γ point in GaN as determined from reflectance data. Group theory (C_{6v}) indicates that σ -polarized optical transitions are allowed for the A, B, and C excitons, but that π -polarized transitions are only allowed for B and C. The relative intensities for the polarized optical transitions, calculated from the quasicubic model with the parameters shown, are indicated in brackets.

ductors have valence-band maxima at $k=0$, the Γ point (if small linear k terms are neglected). In the wurtzite structure, with C_{6v} symmetry at the Γ point, the valence and conduction bands have the symmetries indicated in Fig. 4. We will consider additional complications below, but to begin, let us take the simple case in which there is one exciton transition for each of the three valence states (and assume classical optics applies). Conventionally these are referred to as the A, B, and C excitons as indicated in Fig. 4. The group-theoretical selection rules, shown in Fig. 4, require that the A excitons ($\Gamma_9^v \rightarrow \Gamma_7^c$) appear only for σ and α polarization ($E \perp c$).

We see that the σ and π data in Fig. 3 do consist of three transitions which obey the selection rules in Fig. 4. (For classical optics, α should be identical with σ . The fact that this is not observed is discussed below.) In π polarization, the A exciton is absent and the B and C excitons are well resolved. In σ polarization, the C exciton is weaker, but still well resolved. The A and B excitons overlap in σ but the B exciton is still clearly present. This confirms that GaN has the "normal" ordering of the valence-band states in which the $\Gamma_9^v \rightarrow \Gamma_7^c$ transition energy is smallest.

At this point we apply Hopfield's⁹ quasicubic model to obtain the spin-orbit parameter Δ_{so} , the crystal field parameter Δ_{cr} , and compare the observed polarization intensities with the calculated values. The energy splittings of the valence states are given by

$$\delta E = \frac{1}{2}(\Delta_{so} + \Delta_{cr}) \pm \frac{1}{2}[(\Delta_{so} + \Delta_{cr})^2 - \frac{8}{3}\Delta_{so}\Delta_{cr}]^{1/2}, \quad (1)$$

where the plus (minus) sign refers to the splitting between the Γ_9^v and the lower (upper) Γ_7^v state. We find that the calculated parameter Δ_{so} is quite sensitive to the A-B exciton splitting. Experimentally, we are not able to determine the energies of the three transitions to an accuracy greater than ± 2 meV. (There is some variation with sample. Beyond this it is not a trivial matter to determine the transition energy for reflectance structure affected by spatial dispersion and longitudinal-transverse exciton splitting.) Our best estimate for the A exciton energy is 3.474 ± 0.002 eV. We estimate the valence-band parameters to be $\Delta_{so} = 11 \pm \frac{1}{2}$ meV and $\Delta_{cr} = 22 \pm 2$ meV.

Because Eq. (1) is symmetric in Δ_{so} and Δ_{cr} , we have to consider the intensities in order to distinguish between the two parameters. The values in the brackets in Fig. 4 are the relative theoretical transition intensities for the parameters shown (assuming the matrix elements of P_z equal those for P_x and P_y). We have not made a quantitative comparison with experiment, but there is qualitative agreement. If Δ_{cr} and Δ_{so} were interchanged, the theory predicts approximately equal intensities

for the B and C excitons in π polarization, which clearly conflicts with the data.

The simplified model which we have used gives a rather good account of the over-all features of the data. However, previous work on other materials, such as CdS,^{10,11} has shown that observable structure can arise from other sources.

Here we review some of these effects and attempt to estimate their importance in GaN. First of all, each valence band generates a hydrogenic series of exciton states.¹² Although the optical strength of these transitions is proportional to n^{-3} , $n=2$ (and $n=3$ in CdS) excitons are seen in several II-VI semiconductors. The exciton binding energy has not been measured in GaN, but Dingle and Ilegems¹³ have estimated an effective-mass value of 28–31 meV. Thus the $n=2$ transition should be approximately 22 meV above the $n=1$ state for each exciton series. Such transitions are not apparent in the σ and π spectra. There is structure in α approximately 22 meV above the A exciton, but the absence of comparable structure in σ suggests that it is not the $n=2$ state of the A exciton.

Spatial dispersion can also affect the reflectance spectrum.¹⁰ Two (related) effects have been seen previously. The finite mass of the exciton and the surface boundary conditions can strongly modify the reflectance structure from that expected for a classical oscillator. Also, an additional sharp structure can arise near the longitudinal exciton energy. Generally speaking, these effects are quite important if the natural broadening of the ϵ_2 spectrum is small compared with the longitudinal-transverse exciton splitting and become considerably less important as the natural broadening becomes greater than this splitting. A simple estimate based upon the theoretical absorption strength of the $n=1$ excitons indicates that the longitudinal-transverse exciton splitting should be ≤ 2 meV in GaN. In our best crystals, the observed peak-to-peak widths are approximately 5 meV. This suggests that the observed width results primarily from broadening of ϵ_2 rather than from the "apparent" broadening that can arise from spatial dispersion. For the σ and π reflectance, the observed shapes are essentially the shapes expected for classical optics and no "extra" peaks are seen.

To this point, we have judiciously avoided detailed remarks about the α spectrum. It is seen that the α and σ spectra are not the same, particularly in the 3.48–3.51-eV region. There are two possible explanations: (a) The surface conditions are different for σ and α (one is an irregularly cleaved surface, the other an as-grown surface); (b) spatial dispersion effects are important. Since the structures are comparably sharp in α and σ , we doubt that the surface condition can account for the differences. On the other hand, we cannot convincingly argue that this difference is due to spatial

dispersion. It should be noted, however, that spatial dispersion effects in CdS are greater in α than in σ .¹⁰ A further study of these effects will have to be postponed until better-quality crystals with sharper structure become available.

Finally, structure has been seen in the σ spectrum for the B exciton in CdS which arises from linear k terms in the valence-band energies.¹⁴ Our spectra in GaN are considerably broader than those in CdS and such effects are not observed.

Broad, weak structure is present near 3.56 eV for σ and α polarization, and near 3.58 eV for π polarization. We believe that this structure arises from phonon-assisted transitions involving the 90-meV LO phonon which is seen in the donor-acceptor pair luminescence spectra.¹³ In both luminescence and reflectance it is seen that the phonon-assisted transitions have the same polarization behavior as the parent no-phonon line.

V. LUMINESCENCE SPECTRA

Luminescence¹⁵ from type-I layers always exhibits the features shown in Fig. 5. Typical spectra from type-II and type-III layers are shown in Fig. 6.

Several contrasting features of these data deserve discussion. The type-I layers always exhibit a sharp, high-energy cutoff close to 3.470 eV in their emission spectra. In contrast, the emission from type-II and type-III layers may extend 100 meV to higher energies, even though the prominent peak near 3.467 eV may occur in both cases.

Another feature, essentially absent from type-I layers but very often present in type-II layers, is the band near 3.43 eV. The energy of this feature is not constant, and we have observed it in the range 3.435–3.420 eV. Its origin remains to be estab-

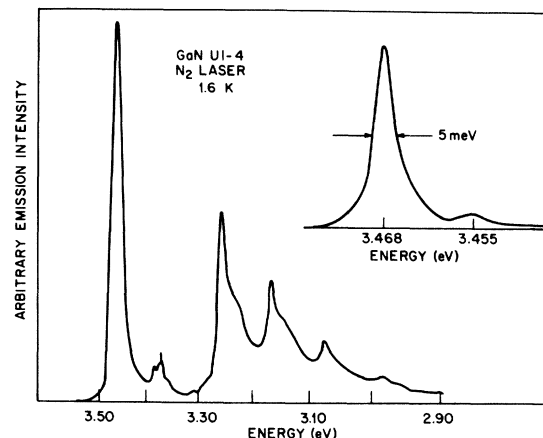


FIG. 5. Typical photoluminescence spectrum of type-I GaN at 1.6 K. The insert is a more detailed view of the strong high-energy peak near 3.468 eV, taken with low excitation intensity and high resolution.

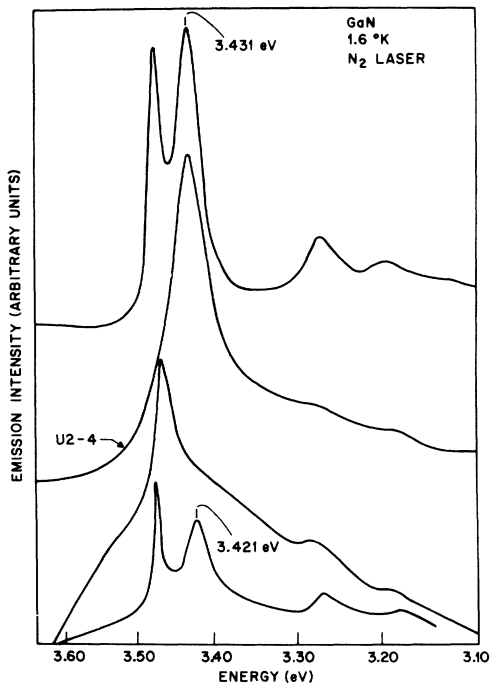


FIG. 6. Typical photoluminescence spectra of type-II and type-III GaN at low temperatures. Three features are worth noting: First, the 3.435–3.42-eV band, which is independent of the presence of the 3.467-eV band, is very prominent; second, luminescence is seen to extend well above the ~ 3.47 -eV cutoff observed in the type-I spectra; finally, only broad, poorly resolved DA pair spectra are evident.

lished.

At lower energies yet, weak structure often occurs near 3.38 eV (type I) in addition to the distant donor-acceptor (DA) recombination spectra recently described and analyzed by Dingle and Ilegems.¹³ The DA bands *always* occur in type-I layers but are often totally absent from type-II and -III spectra. As a final comment upon the spectra of type-III layers (which will not be considered in any detail in this paper), we mention that they are quite similar to the spectra from single-crystal needles reported by us earlier.¹ Moreover, they appear to suffer from the same affliction as did the earlier spectra, namely, that the high free-carrier concentration leads to such a distortion of the absorption and reflectance that the spectra may no longer be considered as characteristic of "pure" GaN.

The spectra shown in Fig. 5 are obtained from front-illuminated layers in which the unique crystal c axis is normal to the layer. These spectra are thus characteristic of the α geometry, and polarization is neither expected nor observed. When these layers (and substrates) are split normal to this face, σ and π data may be obtained (Fig. 7). If due allowance is made for the roughness and

probable depolarizing nature of these surfaces, it is seen that the whole uv spectrum is effectively σ polarized at low temperature (< 2 K). Comparison with CdS and other "normal" wurtzite crystals, as well as a correlation with the presently reported polarization behavior of the reflectance, demonstrates that this anisotropy is quite consistent with an uppermost valence band of Γ_9 symmetry.

In this context, we point out that the weak emission in the π spectrum of Fig. 7 does not occur at precisely the same energy as the major σ emission. In a range of type-I layers, the π component lies 3–5 meV above the σ peak. At present we do not have a detailed understanding of this observation. One possibility is that the excitons are not in thermal equilibrium with the lattice,¹⁶ which we feel sure is at < 2 K, and the π emission could be associated with states derived from the B exciton. This suggestion is consistent with the energies and polarizations deduced from our reflectivity studies, as well as with the fact that we have used intense, short pulses of photons to excite the emission.

Since the layers are always n type, and because the donor-acceptor pair spectra do not dominate, we expect neutral donors to be the most common extrinsic center in the crystals. The pulsed excitation that we use to excite the crystals is known to favor exciton formation, and therefore also bound-exciton emission at low temperatures. From the reflectivity data, the lowest free-exciton energy is 3.474 ± 0.002 eV. The primary emission band falls at 3.466–3.468 eV. By analogy with the well-studied CdS emission spectrum,¹⁷ we denote this band I_2 , and suggest that it arises from the annihilation of excitons bound to neutral donors. This places the exciton localization energy $E_{\oplus+}$ in the region of 6–8 meV. Using the previously deter-

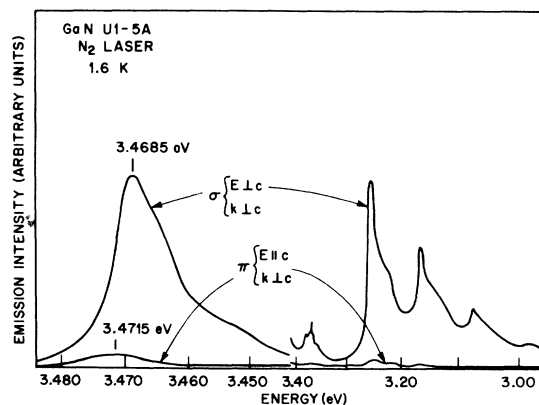


FIG. 7. Polarized photoluminescence spectra of a type-I GaN layer at 1.6 K. The energy scales on the two halves of the figure are not the same. Apart from the very weak 3.4715-eV feature in π , the spectrum is totally σ polarized.

mined¹³ donor binding energy $E_D = 42 \pm 1$ meV, $E_{\ominus_{\pm}}/E_D$ becomes 0.15–0.20, in good agreement with the Haynes rule.¹⁸

In some type-I layers, notably U1-4 and U1-5 shown in Figs. 5 and 7, respectively, there is further weak structure on the low-energy side of the main line. Concentrating on the inset in Fig. 5, we find a weak line at 3.455 eV. Extending the analogy with CdS, and noting the presence of fairly strong distant donor-acceptor pair recombination in this spectrum, we propose to call this line I_1 , and to associate it with an exciton decaying at a neutral acceptor. Applying the Haynes rule¹⁸ ($E_{\ominus_{\pm}}/E_A \sim 0.1$) results in $E_A \sim 190$ meV, in very good agreement with the value of $E_A \sim 200$ meV derived from independent experiments¹³ on the DA pair spectra. Lifetimes measured in the region of these I_1 and I_2 lines are very short¹³ and are thus consistent with the above bound-exciton hypothesis for the 3.467- and 3.455-eV lines.

The weak structure near 3.38 eV has been observed to exhibit two different profiles. The first kind, shown in the lower half of Fig. 8, is very similar to that reported by Pankove *et al.*,¹⁹ although we find the temperature dependence to be quite different from that reported in Ref. 19. At low temperatures we observe a broadened line at 3.3847 eV and a sharp line at 3.3716 eV. The second kind of spectrum found in this region is shown in the upper portion of Fig. 8. It is readily apparent that the sharp 3.3716-eV line is absent.

We believe that the sharp line at 3.3716 eV and the pair of broader lines at 3.3858 and 3.3780 eV are not related. Moreover, since the 3.3716-eV line appears in only some crystals, its origin is also independent of the strong 3.467 ± 0.001 -eV line. The 3.3858- and 3.3780-eV features (and their LO replicas at 3.2934 and 3.2870 eV) are, we believe, intimately connected with the 3.467 ± 0.001 -eV line. Thus, varying the excitation level at low temperatures gives rise to similar changes

in the intensities in the emission at 3.467, 3.38, and 3.29 eV, while the relative intensities of these lines remain in a constant ratio for changes of 10^2 in excitation intensity. More important is the observation that the addition of one LO phonon to the doublet at 3.38 eV produces energies 3.4758 and 3.4680 eV, in close agreement with the energy of the free exciton (3.474 ± 0.002 eV) and the energy of the main photoluminescence peak (3.4680 eV), respectively.

Thus we suggest that the regularly appearing doublet features at 3.38 and 3.29 eV are LO-phonon replicas of the lowest free exciton and of bound excitons decaying at neutral donors, and that the 7.8-meV splitting measured at 3.38 eV is the localization energy of the bound exciton. These results are in agreement with the reflectance and higher-energy photoluminescence data. At present we do not have an assignment for the transition, nor an identification of the chemical nature of the center responsible for the 3.3716-eV line.

The only remaining features in the uv spectrum are the DA pair bands previously discussed by Dingle and Ilegems.¹³ Our understanding of these spectra has not advanced beyond the description given at that time. Consequently, the chemical identity of the involved donors and acceptors remains unknown. What we have discovered, however, is that the peak energy of the no-phonon band does vary from layer to layer. This variation has been found to be as much as 10 meV. Although variations in the concentration of defects or excitation intensity can bring about such a change, we question whether the variation is not due to the presence of donors or acceptors with slightly different binding energies. Certainly, the principal emission band at 3.467 eV varies by 2 or 3 meV from layer to layer and this would scale up to ~ 10 meV for the change in the associated donor binding energy. One final observation, which proves that such variations are possible, is that we have found layers in which a new DA pairlike system appears some 25 meV above the usual DA no-phonon energy, with both DA spectra appearing in the same layer. In this case we expect, but have not been able to prove, that there are two different acceptors present in the layer.

VI. CONCLUSIONS

We have made use of absorption, reflection, luminescence, and electrical measurements, both as monitors of the quality of as-grown layers of GaN as well as probes to examine the physics of the better-quality layers. The absorption and especially the reflectance data have shown quite conclusively that epitaxial GaN is a direct-gap semiconductor with a "normal" $\Gamma_9 > \Gamma_7 > \Gamma_7$ valence-band ordering. As might be expected from the ionic nature of the

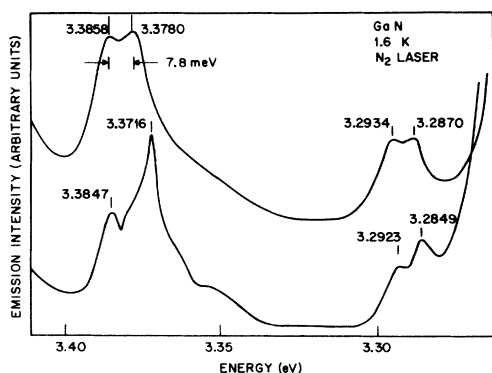


FIG. 8. Two examples of photoluminescence spectra seen in the 3.38- and 3.29-eV regions in type-I layers.

lattice (or the position of the anion in the Periodic Table), the spin-orbit interaction is relatively small ($\Delta_{so} \sim 11$ meV). The "normal" ordering of the spin-orbit split components emphasizes the unique nature²⁰ of the valence band in ZnO and its apparent dependence upon the energy of the Zn *d* bands. Although there is some evidence for further fine structure in the reflectance, its analysis, which should not change the basic conclusions reached here, must await the availability of even better-quality materials.

We have identified weak structure in the luminescence as due to the decay of a free exciton with the simultaneous creation of a photon and one or two LO phonons. The dominant emission peak at 3.467

± 0.001 eV is confidently associated with an exciton decaying at a donor site (I_2), whereas a much more tentative association is made of the weak line at 3.455 eV with an exciton decaying at a neutral acceptor (I_1). Distant donor-acceptor pair spectra complete the near-gap emission.

ACKNOWLEDGMENTS

The authors are particularly indebted to J. J. Hopfield for illuminating discussions on the reflectivity data, to C. H. Henry and J. E. Rowe for helpful comments, to H. C. Montgomery for the electrical measurements, and to K. F. Rodgers, Jr. for assistance with the emission experiments.

¹R. Dingle, D. D. Sell, S. E. Stokowski, P. J. Dean, and R. B. Zetterstrom, *Phys. Rev. B* **3**, 497 (1971).

²R. Dingle, K. L. Shaklee, R. F. Leheny, and R. B. Zetterstrom, *Appl. Phys. Letters* (to be published).

³J. O. Dimmock, in *II-VI Semiconducting Compounds*, edited by D. G. Thomas (Benjamin, New York, 1967), p. 277.

⁴M. Ilegems, *J. Crystal Growth* (to be published).

⁵B. B. Kosicki and D. Kahng, *J. Vac. Sci. Technol.* **6**, 593 (1969).

⁶E. I. Rashba and G. E. Gurgenishvili, *Fiz. Tverd. Tela* **4**, 1029 (1962) [*Sov. Phys. Solid State* **4**, 759 (1962)].

⁷D. D. Sell and P. Lawaetz, *Phys. Rev. Letters* **26**, 311 (1971).

⁸D. D. Sell, *Appl. Opt.* **9**, 1926 (1970).

⁹J. J. Hopfield, *J. Phys. Chem. Solids* **15**, 97 (1960).

¹⁰J. J. Hopfield and D. G. Thomas, *Phys. Rev.* **132**, 563 (1963); *J. J. Hopfield, J. Phys. Soc. Japan Suppl.* **21**, 77 (1966).

¹¹D. G. Thomas and J. J. Hopfield, *Phys. Rev.* **116**, 573 (1959).

¹²A. Baldereschi and M. G. Diaz, *Nuovo Cimento* **68B**, 217 (1970).

¹³R. Dingle and M. Ilegems, *Solid State Commun.* **9**, 175 (1971).

¹⁴G. D. Mahan and J. J. Hopfield, *Phys. Rev.* **135**, A428 (1964).

¹⁵All emission spectra discussed in this paper were obtained with an N₂-gas laser as excitation source. The technique used has been described earlier [R. Dingle, *Phys. Rev.* **184**, 788 (1969)]. Unless specifically stated, all spectra were obtained with the sample immersed in liquid helium either at 4.2 or 1.6 K.

¹⁶A number of recent observations in other semiconductors are consistent with this idea. See, for example, E. Gross, S. Permogorov, V. Travnikov, and A. Selkin, *J. Phys. Chem. Solids* **31**, 2595 (1970).

¹⁷D. G. Thomas and J. J. Hopfield, *Phys. Rev.* **128**, 2135 (1962).

¹⁸See, for example, R. E. Halsted and M. Aven, *Phys. Rev. Letters* **14**, 64 (1965).

¹⁹J. I. Pankove, J. E. Berkeyheiser, H. P. Maruska, and J. Wittke, *Solid State Commun.* **8**, 1051 (1970); J. I. Pankove, H. P. Maruska, and J. E. Berkeyheiser, in *Proceedings of the Tenth International Conference on the Physics of Semiconductors*, edited by S. P. Keller, J. C. Hensel, and F. Stern (U. S. AEC, Oak Ridge, Tenn., 1970), p. 593.

²⁰D. G. Thomas, *J. Phys. Chem. Solids* **15**, 86 (1960); W. Y. Liang and A. D. Yoffe, *Phys. Rev. Letters* **20**, 59 (1968).

Piezoelectricity under Hydrostatic Pressure

James W. F. Woo

IBM Thomas J. Watson Research Center, Yorktown Heights, New York 10598

(Received 16 September 1970)

Phillips's theory of ionicity is used to estimate the piezoelectric coefficient under hydrostatic pressure of several semiconductors with a zinc-blende structure. It is found that this new effect is comparable in magnitude to the usual piezoelectric effect.

In 1960, Landauer¹ pointed out that the classical theory of pyroelectricity, which relates the existence or nonexistence of the pyroelectric effect to

the symmetry of the crystal class, cannot be completely correct. Landauer points out that the presence of boundaries on the crystal breaks the sym-